

# Comparison of Information Extracted from High and Very High Resolution Satellite Images for Update of a GIS

D.Amarsaikhan, M.Ganzorig and B.Nergui

Institute of Informatics, Mongolian Academy of Sciences,  
av.Enkhtaivan-54B, Ulaanbaatar-51, Mongolia  
Tel: 976-11-453660, Fax: 976-11-458090

**Abstract**—The aim of this study is to compare the information extracted from high and very high resolution satellite images in terms of information content and reliability to update thematic layers in a geographical information system (GIS). For the extraction of information from the selected remote sensing (RS) data sets, a knowledge-based classification technique based on a rule-based approach has been constructed. The method uses an initial image segmentation procedure based on a Mahalanobis distance classifier (or spectral parameters) as well as the constraints on spectral and spatial thresholds. Overall, the study indicated that unlike the information extracted from high resolution RS images which contains large uncertainty in terms of delineation of individual objects, the information extracted from very high resolution satellite images are very reliable and can be successfully used for update of a GIS layer specifically in urban context.

## I. INTRODUCTION

Until the launch of very high resolution satellites such as Ikonos and Quickbird, space data sets had been mainly used for a land cover mapping at regional or smaller scales, because the available high resolution satellite images (e.g., Landsat and SPOT) could fulfill the mapping conditions of only regional level. As it is known, the scale of the thematic information to be extracted from digital RS data is dependent upon the spatial resolution of the acquired images. To get an acceptable accuracy for the selected map scale using optical images it is desirable to include at least 20-25 pixels per centimeter, however, these numbers may change depending on the purposes of the study as well as the requirements of conducted projects [3]. The standard high resolution satellite data sets allow the mapping specialists to map the natural and man made features usually at a class level and it is very difficult to define the individual objects on such images. However, using very high resolution RS images it is possible to map any features at object as well as class levels.

Traditionally, the results of satellite RS image analysis have been used for update of different thematic layers in a GIS at national and regional levels [1,2]. As the current very high resolution satellite data sets allow the users of spatial information to map the features at an object level, it is possible to update the layers of a GIS at all levels including national, regional and local. Cartographers often divide the maps into three different categories such as small-scale maps that use scales smaller than 1: 250,000, intermediate-scale maps that use scales between 1:50,000 and 1:250,000 and large-scale maps that use scales larger than 1:50,000 (Map Scale). The database levels in a GIS cannot be directly related to these map scales, because different GIS users use different map scales for determination of the levels. However, as all spatial

databases are based on map scales there can be a relationship between the levels and scales [2]. For example, national level can be referred to small to medium scales, regional level can be referred to medium to large scales and local level can be referred to only large scale, depending on the used data sources.

Over the years, for the extraction of thematic information from RS images at national and regional levels, different image processing techniques have been used. Most of these techniques were based on digital methods of classification which mainly included statistical and non-statistical methods, neural networks as well as other knowledge-based classifications [1,5,9,12]. In recent years, for identification of the individual objects different object-oriented classification techniques have been used [10,13].

The aim of this study is to compare the information extracted from the high and very high resolution RS images in terms of the information content and reliability to update a GIS layer. Generally, urban areas include complex and diverse environments, in which many features have similar spectral characteristics and it is not easy to separate them by the use of ordinary feature combinations or by applying standard techniques [5]. In the present study, for identification of available urban land-cover types a knowledge-based classification technique based on a rule-based approach has been constructed. The constructed method uses an initial image segmentation procedure based on a Mahalanobis distance classifier (or spectral parameters) as well as the constraints on spectral and spatial thresholds. The results of the knowledge-based method were compared with results of a statistical maximum likelihood classification (MLC) and they demonstrated higher accuracies. As a test site, Ulaanbaatar, the capital city of Mongolia has been selected and as RS data sources Landsat ETM(+) data as well as Quickbird and SPOT 5 images have been used.

## II. TEST SITE AND DATA SOURCES

As a test site, Baga toiruu area situated in central part of Ulaanbaatar, the capital city of Mongolia has been selected. The Baga toiruu is the city business district of Ulaanbaatar city where different government, educational, cultural and commercial organizations are located. Besides the Central Government, Parliament and headquarters of major political parties, the Baga toiruu contains approximately two third of ministries, one third of major government organizations, half of bank headquarters, one fifth of all state universities, half of diplomatic and international organizations, and many

theatres and museums [6]. The location of the Baga toiruu area represented in a Quickbird image of 2002 is shown in figure 1.



Figure 1. The test area represented in a Quickbird image of 2002.

As the RS data sources, multispectral SPOT 5 image of 2002 resampled to a pixel resolution of 4m and Quickbird image of 2002 with a spatial resolution of 70cm, and Landsat ETM (+) data of 2001 have been used. The ETM(+) data consisted of a panchromatic band resampled to a pixel resolution of 14m and multispectral bands (except bands 61 and 62) resampled to a pixel resolution of 28m. In addition, a topographic map of 1984, scale 1:50 000 and a topographic map of 2000, scale 1:5 000 as well as GIS layers created on the basis of the topographic maps, were available.

### III. RADIOMETRIC CORRECTION AND GEOREFERENCING OF THE PANCHROMATIC AND MULTISPECTRAL IMAGES

At the beginning, all the available images were thoroughly analyzed in terms of radiometric quality and geometric distortion. The panchromatic band of the ETM(+) data had some radiometric noise and it was corrected by applying a 3x3 size average filter [11]. Moreover, band 1 of the ETM(+) data had high atmospheric noise and it was decided to be excluded from the further analysis. The Quickbird data had some shadows of buildings and for the reduction of the shadows a topographic normalization [8] has been carried out.

In order to extract geometrically accurate thematic information, thorough georeferencing should be applied to the original RS images. Initially, the Quickbird image has been georeferenced to a Gauss-Kruger map projection using a topographic map of 2000, scale 1:5 000. The ground control points (GCP) have been selected on well

defined cross sections of roads, streets and building corners and in total, 12 regularly distributed points were selected. For the transformation, a second order transformation and nearest neighbour resampling approach [16] have been applied and the related root mean square (RMS) error was 1.29 pixel. Likewise, the multispectral SPOT 5 image has been georeferenced to a Gauss-Kruger map projection using the same topographic map of the test area. For the transformation the same number of GCPs has been used and the related RMS error was 0.98 pixel. In each case of the georeferencing, an image was resampled to a pixel resolution of 70cm. Then, the panchromatic and multispectral bands of the ETM data were georeferenced to a Gauss-Kruger map projection using a topographic map of 1984, scale 1:50 000. The GCPs have been selected on well defined sites and in total 9 regularly distributed points were selected. For the transformation, a linear transformation and nearest neighbour resampling approach have been applied and the related RMS errors were 0.92 pixel and 0.87 pixel, accordingly. In both cases, an image was resampled to a pixel resolution of 14m.

### IV. EXTRACTION OF INFORMATION AT CLASS AND OBJECT LEVELS

Over the past years, knowledge-based techniques have been widely used for the classification of RS images. The knowledge in image classification can be represented in different forms depending on the type of knowledge and necessity of its usage [4]. The most commonly used techniques for knowledge representation are a rule-based approach and neural network classification [5]. In the present study, for discrimination of the urban land-cover types and available objects a rule-based approach has been applied. A rule-based approach uses a hierarchy of rules, or a decision tree describing the conditions under which a set of low-level primary objects becomes abstracted into a set of the high-level object classes. The primary objects contain the user-defined variables and include geographical objects represented in different structures, external programmes, scalars and spatial models [8].

#### A. Extraction of Information at Class Level

For the extraction of the urban land cover information from the ETM(+) data, a rule-based approach that uses an initial image segmentation based on spectral parameters and other constraints on the spectral and spatial thresholds has been constructed.

The ETM data of the selected part of the capital city is shown in figure 2a. As seen from the figure 2a, the site is characterized by such spectral classes as builtup area (mainly buildings), open area (mainly roads and pedestrian walking areas), central square and vegetation (trees and grass). To extract reliable features, a principal component analysis (PCA) has been performed to the integrated panchromatic and multispectral data sets and the result is shown in table 1.

TABLE 1. PRINCIPAL COMPONENT COEFFICIENTS FROM PANCHROMATIC AND FIVE MULTISPECTRAL BANDS OF THE ETM.

	PC1	PC2	PC3	PC4	PC5	PC6
PAN	0.16	-0.32	-0.92	-0.15	0.02	0.01
ETM2	0.36	0.46	-0.14	0.14	-0.77	0.07

ETM3	0.48	0.58	-0.11	0.08	0.62	0.09
ETM4	0.12	-0.22	-0.04	0.85	0.05	-0.43
ETM5	0.51	-0.48	0.24	0.13	-0.01	0.64
ETM7	0.56	-0.21	0.23	-0.43	-0.04	-0.62
Eigenvalue	973.1	139.9	101.6	24.07	11.44	6.83
Variance (%)	77.41	11.13	8.08	1.9	0.91	0.57

As seen from table 1, in the PC1 that contains 77.41% of the overall variance middle infrared bands have high loadings, whereas in the PC2 that contains 11.13% of the overall variance, variance of the visible red band has a total dominance. In the PC3 that contains 8.08% of the overall variance, panchromatic band has a very high negative loading. Moreover, as seen from the table 1, in the PC4 that contains 1.9% of the overall variance, near infrared band has a very high loading. The inspection of the last two PCs indicated that they contained noise from the total data set. As could be seen, the first 3 PCs contain 96.62% of the overall variance, and one could think that they might have been sufficient for the feature determination. However, visual inspection of the PC 4 indicated that it included useful information related to green vegetation. Therefore, for the final features, PC1, PC2, PC3 and PC4 have been chosen.

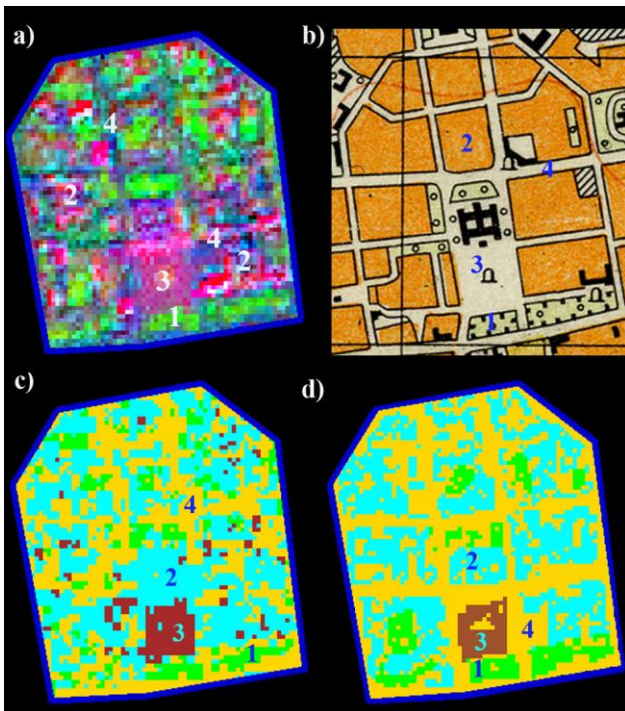


Figure 2. a) ETM image of the test area, b) A topographic map of the test area, c) The result of the MLC, d) The result of the rule-based method. (1-Vegetation, 2-Builtup area, 3-Central square, 4-Open area).

As an initial step to construct the rules, the training signatures have been selected. To define the training signatures from the PCA image, 2–3 areas of interest (AOI) representing the selected four classes have been chosen through accurate analysis based on local knowledge. The separabilities of the training signatures were first checked on the feature space images and then evaluated using Jeffries-Matusita (JM) distance. Then the samples which demonstrated the greatest separabilities were chosen to form the final signatures. The final signatures included about 26–84 pixels. The plot of the

mean values for the chosen signatures in the selected bands is shown in Figure 3.

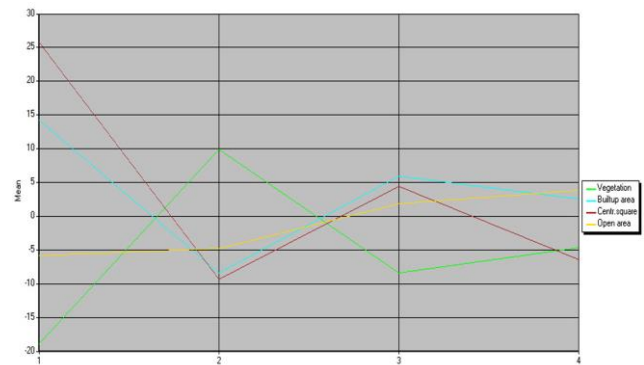


Figure 3. The plot of the mean values for the selected classes in PC bands.

For the initial image segmentation, as the upper and lower limits of the spectral parameters, the values falling mainly within minimum and maximum of each class defined from the selected signatures have been selected. The pixels falling outside of these spectral parameters were temporarily identified as unknown classes and further classified using the rules in which different spectral and spatial thresholds were defined. In general, it is very difficult to separate the classes if they have the same or very similar spectral characteristics. In case of this study, as we have urban environment, there are high mixtures among the classes except the green vegetation.

When the classes overlap in a multidimensional feature space, the usage of thoroughly defined spectral and spatial thresholds can play an important role for separating the overlapping classes. The spectral thresholds can be defined from the statistics of the training signatures of the available classes, while the spatial thresholds can be determined on the basis of GIS data sets or from local knowledge about the site. In this study, the further spectral thresholds were determined based on the pixel values falling between 1.0–1.5 standard deviation (SD) from the mean of each class, whereas the spatial thresholds were determined using the polygon boundaries defined on the basis of a GIS layer (the layer was created from a topographic map of 1:50 000 shown in figure 2b). The final land-cover map was created by a combined use of Spatial Modeler and Knowledge Engineer modules of Erdas Imagine. The flowchart for the constructed rule-based approach is shown in figure 4 and the classified image is shown in figure 2d. For the accuracy assessment of the classification result, the overall performance has been used [7]. As ground truth information, for each class several regions containing the total of 897 purest pixels have been selected. The confusion matrix indicated an overall accuracy of 90.19% (table 2a).

To compare the performances of the developed algorithm and a standard method, the same set of features were classified using the statistical MLC. The image classified by the MLC method is shown in figure 2c. As could be seen from the figure 2c, the classified image has

high mixtures of all classes. The confusion matrix indicated an overall accuracy of 75.36% (table 2b).

TABLE 2a. CONFUSION MATRIX PRODUCED FOR THE CLASSIFIED IMAGE SHOWN IN FIGURE 2D.

Classified data	Reference data			
	Vegetation	Builtup area	Central square	Open area
Vegetation	112	15	0	0
Builtup area	0	312	0	0
Central square	0	0	102	0
Open area	26	32	15	283
Total	138	359	117	283
Overall Accuracy = 90.19% (809/897)				

TABLE 2b. CONFUSION MATRIX PRODUCED FOR THE CLASSIFIED IMAGE SHOWN IN FIGURE 2C.

Classified data	Reference data			
	Vegetation	Builtup area	Central square	Open area
Vegetation	107	16	0	8
Builtup area	0	205	5	12
Central square	0	11	112	11
Open area	31	127	0	252
Total	138	359	117	283
Overall Accuracy = 75.36% (676/897)				

### B. Extraction of Information at Object Level

As we had data sets with different spatial and spectral resolutions, they should be merged for conducting further analyses. In this study, to merge the Quickbird and SPOT 5 images, Brovey transform and PCA [11,17] have been applied and the results were compared. For the Brovey transform, the bands of SPOT 5 were considered as the multispectral bands, while the Quickbird image was considered as the higher spatial resolution band. The PCA has been performed using the available panchromatic and multispectral bands. As it was seen from the PCA, the first three PCs contained almost 98% of the total variance. The inspection of the last PC indicated that it contained noise from the total dataset. Therefore, it was excluded from the analysis.

In order to obtain a reliable image that can illustrate the spectral and spatial variations in the selected classes of objects, different band combinations have been compared. Although, the image created by the Brovey transform contained some shadows that were present on the panchromatic image, it still illustrated good result in terms of separation of the available land use classes and individual objects. The image created by the PCA method contained less shadows, however, it was very difficult to analyze the final image, because it contained too much color variation of objects belonging to the same class. Therefore, for further analysis the image created by the Brovey transform has been used. As seen from the Brovey transformed image shown in figure 4a, all details are clearly seen. For creation of urban GIS layer, the selected classes of objects were screen digitized from the topographic map of 2000 (figure 4b).

To extract the urban land cover information at object level, a rule-based approach which consists of a set of

rules, that contains the initial image segmentation procedure based on a Mahalanobis distance classifier [15] and the constraints on spectral parameters and spatial thresholds, has been constructed. The Mahalanobis distance classifier is a parametric method, in which the criterion to determine the class membership of a pixel is the minimum Mahalanobis distance between the pixel and the class centre.



Figure 4. a) The Brovey transformed image of the test area, b) A topographic map of the test area.

In the Mahalanobis distance estimation, for the initial separation of the classes, only pixels falling within 1.0-1.5 standard deviation (SD) and the Brovey transformed features were used. The pixels falling outside of 1.0-1.5 SD were temporarily identified as unknown classes and further classified using the rules in which different spectral and spatial thresholds were used. The spectral thresholds were determined based on the knowledge about spectral characteristics of the selected classes, whereas the spatial thresholds were determined based on polygon boundaries of the created GIS layer. The image classified by the rule-based approach is shown in figure 5b.

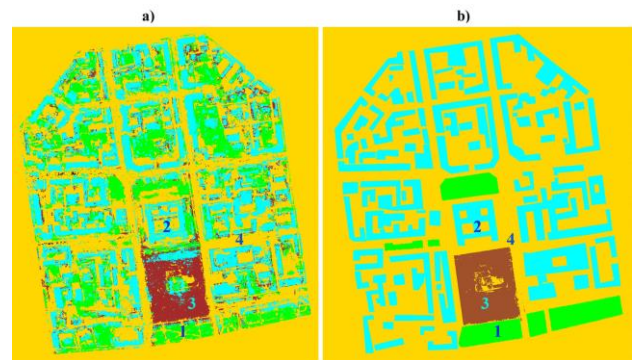


Figure 5. a) The result of the MLC, b) The result of the rule-based method. (1-Vegetation, 2-Builtup area, 3-Central square, 4-Open area).

As seen from the classified image, the rule-based approach could very well separate all individual objects. For the accuracy assessment of the classification result, the overall performance has been used. As ground truth information, for each class several regions containing the total of 3686 purest pixels have been selected. The confusion matrix indicated an overall accuracy of 98.78% (table 3a).

To compare the performances of the developed algorithm and a standard method, the same set of features and training signatures used for the rule-based classification, were classified using the statistical MLC.

The image classified by the MLC method is shown in figure 5a. The confusion matrix indicated an overall accuracy of 86.97% (table 3b).

TABLE 3a. CONFUSION MATRIX PRODUCED FOR THE CLASSIFIED IMAGE SHOWN IN FIGURE 6B.

Classified data	Reference data			
	Vegetation	Builtup area	Central square	Open area
Vegetation	512	0	0	0
Builtup area	0	1426	0	0
Central square	0	0	449	8
Open area	0	0	37	1254
Total	512	1426	486	1262
Overall Accuracy = 98.78% (3641/3686)				

TABLE 3b. CONFUSION MATRIX PRODUCED FOR THE CLASSIFIED IMAGE SHOWN IN FIGURE 6A.

Classified data	Reference data			
	Vegetation	Builtup area	Central square	Open area
Vegetation	437	88	34	107
Builtup area	17	1233	28	0
Central square	0	0	395	14
Open area	58	105	29	1141
Total	512	1426	486	1262
Overall Accuracy = 86.97% (3206/3686)				

### C. Comparison of the Information Extracted at Class and Object Levels for Updating GIS Layers

As seen from the classification results shown in figure 2b-c, the result of the rule-based method looks better than that of the standard method, however, it contains large uncertainty in terms of delineation of individual objects. In general, urban areas comprise complex and diverse environments containing a variety of different features and objects having very similar spectral characteristics and it is not easy to separate them even using sophisticated techniques. In the selected test area, the classes: built-up area, open area and central square have very similar spectral characteristics and there are different mixtures of these classes on the final classified image. Therefore, this result cannot be considered as reliable and surely cannot be used for update of a GIS layer.

Moreover, as seen from the classification results shown in figure 6a-b, the result of the rule-based method looks much better than that of the standard method and the extracted objects are very accurately delineated forming the classes of objects. The comparison of the extracted objects with the existing GIS layer (figure 4b) shows that there had occurred some changes within a two year period. Therefore, the obtained result could be successfully used for update of the GIS layer after making some corrections.

## V. CONCLUSIONS

The aim of this study was to compare the information extracted from the high and very high resolution satellite images of Ulaanbaatar, the capital city of Mongolia in

terms of information content and reliability to update GIS layers. For the extraction of land cover information from the selected RS data sets, a knowledge-based classification technique based on a rule-based approach has been constructed. The constructed method uses an initial image segmentation procedure based on a Mahalanobis distance classifier (or spectral parameters) as well as the constraints on spectral and spatial thresholds. The results of the knowledge-based method were compared with results of a statistical MLC and they demonstrated higher accuracies.

Overall, the study indicated that the information extracted from very high resolution satellite images are very reliable and can be successfully used for update of a GIS layer specifically in urban context. Unlike this case, the information extracted from high resolution satellite images as it contains large uncertainty in terms of delineation of classes and objects, its use for update of a GIS layer is very much dependent on the accuracy of the obtained thematic information as well as the update requirements of a given GIS.

## REFERENCES

- [1] D.Amarsaikhan, "Update of a GIS by RS data using a knowledge-based approach", *PhD Dissertation*, Mongolian Academy of Sciences, 1996, pp.150.
- [2] D.Amarsaikhan, "Update of a GIS by methods of RS", *Erdem Newsletter of the MAS*, No.4, pp.12-16, 2002.
- [3] D.Amarsaikhan and M.Sato, "The role of high resolution satellite images for urban area mapping in Mongolia", In *Reviewed Papers' part of Proceedings of the Computers for Urban Planning and Urban Management (CUPUM)'03 International Conference*, Sendai, Japan, pp.1-12, 2003.
- [4] D.Amarsaikhan and T.Douglas, "Data fusion and multisource data classification", *International Journal of Remote Sensing*, Vol.17, pp. 3529-3539, 2004.
- [5] D.Amarsaikhan, M.Ganzorig, P.Ache and H.Blotevogel, "The Integrated Use of Optical and InSAR Data for Urban Land Cover Mapping", *International Journal of Remote Sensing*, 28, pp.1161-1171, 2007.
- [6] B.Chinbat, M.Bayantur and D.Amarsaikhan, "Investigation of the internal structure changes of Ulaanbaatar city using RS and GIS", *Proceedings of the ISPRS Mid-term Symposium*, ITC, Enschede, The Netherlands, 2006.
- [7] ENVI, User's Guide, Research Systems, USA, 1999.
- [8] ERDAS, Field guide, Fifth Edition, ERDAS, Inc. Atlanta, Georgia, 1999.
- [9] P.Gamba and B.Houshmand, "An efficient neural classification chain of SAR and optical urban images". *IEEE Transactions on Geoscience and Remote Sensing*, Vol.22, 1535-1553, 2001.
- [10] S.Giada, T.D.Groove, D.Ehrlich and P.Soille, "Information extraction from very high resolution satellite imagery over Lukole refugee camp, Tanzania", *International Journal of Remote Sensing*, Vol.24, pp.4251-4266, 2003.
- [11] R.C.Gonzalez and R.E.Woods, *Digital Image Processing*, Second Edition, Upper Saddle River, (New Jersey: Prentice-Hall), 2002.
- [12] M.Linderman, J.Liu, J.Qi, L.An, Z.Ouyang, J.Yang and Y.Tan, "Using artificial neural networks to map the spatial distribution of understory bamboo from remote sensing data". *International Journal of Remote Sensing*, Vol.25, pp. 1685-1700, 2004.
- [13] V.L.Lucier, "Object-oriented classification of sidescan sonar data for mapping benthic marine habitats", *International Journal of Remote Sensing*, 29, pp.905 - 921, 2008.
- [14] Map scale - measuring distance on map, available at: <http://geography.about.com/cs/maps/a/mapscale.htm>.
- [15] P.M.Mather, *Computer Processing of Remotely-Sensed Images: An Introduction*, Second Edition, (Wiley, John & Sons), 1999.
- [16] J.A.Richards and X.Jia, *Remote Sensing Digital Image Analysis-An Introduction*, Third Edition, (Berlin: Springer-Verlag), 1999.

- [17] J.Vrabel, "Multispectral imagery band sharpening study".  
*Photogrammetric Engineering and Remote Sensing*, Vol.62,  
pp.1075-1083, 1996.